European Radiology (2019) 29:4207–4214
https://doi.org/10.1007/s00330-018-5762-y

COMPUTED TOMOGRAPHY

Comparison of dual- and single-source dual-energy CT in head and neck imaging

Matthias Stefan May[1] · Marco Wiesmueller[1] · Rafael Heiss[1] · Michael Brand[1] · Joscha Bruegel[1] · Michael Uder[1] · Wolfgang Wuest[1]

Received: 22 June 2018 / Revised: 22 August 2018 / Accepted: 13 September 2018 / Published online: 18 October 2018

Abstract

Objectives The aim of this study was to compare image quality of single-source dual-energy CT (SS-DECT) with third-generation dual-source dual-energy CT (DS-DECT) in head and neck cancer.

Materials and methods One hundred two patients with histologically proven head and neck cancer were prospectively randomized to undergo radiation dose-matched SS-DECT ($n = 51$, 120 kV, split-filter technique, 384 ref. mAs) or DS-DECT ($n = 51$, 80/Sn150 kV, tube A 100/tube B 67 ref. mAs). Inline default images (DI) and virtual monoenergetic images (VMI) for two different low energies (40 and 60 keV) were reconstructed. Objective image quality was evaluated as dose-normalized contrast to noise ratio (CNRD), and subjective image quality was rated on a 5-point Likert scale.

Results In both groups, highest CNRD values for vessel and tumor attenuation were obtained at 40 keV. DS-DECT was significantly better than SS-DECT regarding vessel and tumor attenuation. Overall subjective image quality in the SS-DECT group was highest on the DI followed by 40 keV and 60 keV. In the DS-DECT group, subjective image quality was highest at 40 keV followed by 60 keV and the DI. Forty kiloelectron volts and 60 keV were significantly better in the DS-DECT compared to the SS-DECT group (both $p < 0.01$).

Conclusions In split-filter SS-DECT as well as in DS-DECT, highest overall image quality in head and neck imaging can be obtained with a combination of DI and low keV reconstructions. DS-DECT is superior to split-filter SS-DECT in terms of subjective image quality and vessel and tumor attenuation.

Key Points

- *Image quality was diagnostic with both dual-energy techniques; however, the dual-source technique delivered significantly better results.*
- *Highest overall image quality in head and neck imaging can be obtained with a combination of default images and low keV reconstructions with both dual-energy techniques.*
- *The results of this study may have relevance for the decision-making process regarding replacement of CT scanners and focused patient examination considering image quality and subsequent therapeutic decision-making.*

Keywords Diagnostic imaging · Head and neck neoplasms · Image enhancement

Abbreviations

A	Mean attenuation
CNR	Contrast to noise ratio
DI	Default image
DLP	Dose-length product
DS-DECT	Dual-source dual-energy CT
ED	Effective radiation dose
HU	Hounsfield units
keV	Energy levels
N	Image noise
SS-DECT	Single-source dual-energy CT
ROIs	Regions of interest
VMI	Virtual monoenergetic images

✉ Wolfgang Wuest
wolfgang.wuest@uk-erlangen.de

[1] Department of Radiology, University Hospital Erlangen, Maximiliansplatz 3, 91054 Erlangen, Germany

Introduction

CT is a crucial imaging method for the head and neck region due to its wide availability, relatively low costs, and very short scan time. As contrast medium is almost always needed for oncologic indications, different technical approaches are available to increase image quality by increasing the contrast to noise ratio. Dual-energy technique provides inline default images (DI) with image quality comparable to conventional single-energy examinations and additionally allows for various post-processing applications [1]. One option is to reconstruct different predicted low energy levels (keV), called virtual monochromatic images (VMI), in order to increase the image contrast. The closer the virtual photon energy approaches the k-edge of iodine at 33 keV, the higher the iodine contrast, albeit at the expense of increased image noise [2]. However, as previously shown, the contrast to noise ratio is increased at low-energy VMI which are therefore suitable for soft tissue imaging [3].

Most of the published studies covering dual energy in the head and neck region used dual-source CT scanners [4, 5].

For single-source CT, different vendors provide different technical approaches to obtain dual-energy data: double spiral acquisitions, fast kilovolt-switching, dual-layer detectors, or split-filter technique [6–9]. As hardware, acquisition, and post-processing vary between the different vendors, comparability between these different systems is limited and it remains unclear which technique should be used. All commercially available DECT techniques have its strengths and weaknesses [2]. DS-DECT for example suffers from a limited field of view (268–353 mm) because of incomplete coverage from the smaller detector. However, the limited FOV is not entirely relevant for imaging the head and neck region and DS-DECT provides the highest spectral separation and could therefore be considered as reference for soft tissue iodine discrimination [6].

The split-filter technique for single-source dual-energy CT (SS-DECT) was recently introduced from the same vendor as DS-DECT, and it is unclear how these two different techniques compare to each other.

The aim of this study was therefore to investigate the effect of SS-DECT on image quality of inline DI and post-processed VMI in patients with head and neck cancer and to compare them to DS-DECT examinations from the same vendor.

Materials and methods

Consecutive patients with histologically proven head and neck cancer scheduled for staging CT were screened for study participation. After sample size calculation, a total of 102 patients were included in the study between January 2015 and January 2016.

Patients were assigned to either the SS-DECT study group or the DS-DECT reference group by random allocation.

Contraindications for CT imaging were known allergies to iodinated contrast material, pregnancy, and impaired renal function (estimated glomerular filtration rate below 45 mL/min). Exclusion criteria for this study were age younger than 18 years and non-contrast studies. All patients signed written informed consent. The study protocol was approved by the local Institutional Review Board and applies to the HIPAA criteria and the Declaration of Helsinki.

The arms were lowered and placed beneath the trunk in both groups for the examination of the neck. After the localizer, 100 mL contrast medium (350 mg iodine/mL, Imeron; Bracco) was injected at a flow rate of 3 mL/s, followed by a saline bolus (30 mL, 3 mL/s). The dual-energy examination was performed with a delay of 80 s in all patients. Scan parameter settings of both groups are given in Table 1. In both groups, real-time automatic tube current modulation software (CareDose4D; Siemens Healthineers) was used to individually adjust the radiation exposure to the patient's anatomy.

A 16-cm phantom with a probe containing 35 mg iodine per milliliter in the center was scanned on both DECT platforms and post-processed the same way as the patient images.

Single-source DECT

All SS-DSCT examinations were performed using a third-generation 128 slice scanner (CT Definition AS+, Siemens Healthcare GmbH) equipped with split-filter technique and a single-layer energy-integrating detector (Stellar, Siemens Healthcare GmbH). Dual-energy data is created by adding a combined gold (50 μm) and tin (600 μm) prefiltration with partial (each 50%) coverage in *z*-axis and full coverage of the field of view (500 mm) to the regular aluminum body filter. Due to the different atomic numbers and attenuations, the 120-kV x-ray beam is separated into a high-energy (after passing the tin filter) and a low-energy (after passing the gold filter) x-ray spectrum [7]. To acquire data from each voxel element with both energy levels, the pitch factor needs to be limited to 0.5 or less [8]. The estimated radiation exposure in the SS-DECT group was matched to the DS-DECT in an ex ante trial using a 16-cm acrylic CTDI phantom by stepwise adjusting the reference tube current time product (384 ref. mAs, Table 1).

Dual-source dual energy

All DS-DECT examinations were performed on a third-generation dual-source CT (Somatom FORCE, Siemens) equipped with two 192 slice energy integrating detectors (Stellar^{Infinitiy}, Siemens Healthcare GmbH). An additional tin prefiltration (600 μm) is added to the standard aluminum body

Table 1 Scan parameters for DS-DECT and SS-DECT groups

Scan parameters	DS-DECT	SS-DECT
kV	Tube A/B 80/150Sn	120
Reference mAs	Tube A/B 100/67	384
Pitch	0.7	0.3
Reconstruction kernel DI	Bf40/Br64	B31/B70
Reconstruction kernel VMI	Qr40	D30
Collimation	192 × 0.6 mm	64 × 0.6 mm
Slice thickness	3 mm	3 mm
Iterative reconstruction	No	No
Rotation time	0.25 s	0.3 s
CTDIvol (mGy)	18.6 ± 3.9	17.1 ± 1.6

SS-DECT single-source dual-energy CT, *DS-DECT* dual-source dual-energy CT, *DI* default images, *VMI* virtual monoenergetic reconstructions

filter for the higher tube-detector system in order to improve the spectral separation (Sn150 kV, Table 1).

Default images

On the basis of the DECT raw data, 3-mm axial DI were reconstructed inline on the console without further post-processing using matching soft and sharp reconstruction kernels. DI in general are intended to provide image quality comparable to conventional single-energy examinations. With SS-DECT spectral weighting in raw data space (C-type reconstruction) and with DS-DECT, a multiband filtered setting (F-type reconstruction 0.7, non-linearly merging 70% of the 80-kVp and 30% of the 150-kVp data spectrum) is available. No iterative reconstructions were used to limit the bias between SS- and DS-DECT.

Virtual monoenergetic images

Thin slices in axial orientation (0.6 mm slice thickness, 0.5 mm increment) were reconstructed separately for the high- and the low-energy spectra from both DE techniques using matching soft DE kernels for further post-processing. All VMI datasets were reconstructed using a dedicated advanced algorithm (Monoenergetic+, Siemens Healthcare GmbH) on a commercially available workstation (SyngoVia VB10, Siemens Healthcare GmbH). This software enables the extrapolation of monoenergetic datasets by linearly scaling both components separately to a specific keV value, ranging from 40 to 190 keV. For soft tissue evaluation, two low monoenergetic image series (40 and 60 keV) were reconstructed (3 mm slice thickness, 3 mm increment) in both groups. High keV series were ruled out as it is well-known that they provide no benefit for examinations with contrast medium and tumor evaluation [1].

Objective image quality

Regions of interest (ROIs) were placed on axial slices in both jugular veins, in both sternocleidomastoid muscles, and in the highest attenuating area of the tumor in order to obtain objective parameters of image quality: mean attenuation (A) in Hounsfield units (HU) and its standard deviation representing image noise (N). The images were reviewed starting with a default soft tissue (center 50 HU/width 400 HU) and bone window (450/1500 HU) that could be adjusted at the reader's discretion. ROIs were drawn blinded to the dual-energy technique and as large as possible, while carefully avoiding adjacent structures and artifacts. Contrast to noise ratio (CNR) was calculated using Eq. 1 and dose-normalized CNR (CNRD) was calculated using Eq. 2 [9].

$$\mathrm{CNR} = (A_{\mathrm{vessel}} - A_{\mathrm{muscle}})/N_{\mathrm{muscle}} \quad (1)$$

$$\mathrm{CNRD} = \mathrm{CNR}/\sqrt{\mathrm{CTDI}_{\mathrm{vol}}} \quad (2)$$

Subjective image quality

Tumor contrast and tumor margins (1 = not visible; 2 = poor, below average; 3 = average, acceptable for clinical use; 4 = very good; 5 = excellent), image artifacts (1 = extensive artifacts, 2 = limited artifacts, 3 = moderate artifacts, 4 = little artifacts, 5 = no artifacts), and overall image quality, not focusing specifically on tumor evaluation (1 = non-diagnostic, 2 = limited, 3 = moderate, 4 = good, 5 = excellent), were independently evaluated by two senior radiologists blinded to all clinical data using 5-point Likert scales. Interreader agreement was assessed based on these results. For comparison of SS-DECT and DS-DECT, only the results from one senior author were taken; no consensus image quality score was established. All presented data in this paper except the interreader agreement are based on the same senior author.

Radiation exposure

The radiation exposure was assessed as $\mathrm{CTDI}_{\mathrm{vol}}$ and dose-length product (DLP) as provided by the scanner. The effective radiation dose (ED) associated with the CT examination was calculated using the following equation: DLP (mGy × cm) × 0.0051 ($\mathrm{mSv} \times \mathrm{mGy}^{-1} \times \mathrm{cm}^{-1}$) [10]. Because SS-DECT examinations are referenced to a 32-cm phantom in the patient protocol, the values had to be converted to match the 16-cm phantom [10]. According to the vendor, the respective conversion factor for the CT system used in this study is 2.0.

Statistical analysis

Sample size calculation was performed using the CNRD results in the jugular veins from the first 20 patients and

following a superiority hypothesis for DS-DECT with a desired statistical power of 90%. Kolmogorov-Smirnov test was used to evaluate the data for normal distribution. In the case of normal distribution, values are given as mean ± standard deviation otherwise as median and range whenever normal distribution was not assumed. In both groups, non-parametric Friedman ANOVA was performed for evaluation of objective and subjective image quality between the different reconstructions as normal distribution was not assumed by Kolmogorov-Smirnov test. Post hoc tests as proposed by Conover were performed for the Friedman ANOVA.

For comparison of objective and subjective image quality and radiation exposure between the SS- and DS-DECT groups, non-parametric Mann-Whitney *U* test was performed as normal distribution was not assumed by Kolmogorov-Smirnov test.

In both groups, interrater agreement was assessed by estimating Cohen's kappa coefficients. Kappa values ≥ 0.41 were interpreted as moderate, kappa values ≥ 0.61 as substantial, and kappa values ≥ 0.81 as almost perfect agreement according to Landis and Koch [11]. Statistical significance level was assumed to be 0.05. Statistical analysis was performed using the software package SPSS Statistics version 21 (SPSS Inc./IBM).

Results

CT examinations

Sample size calculation resulted in a minimum of 47 patients per group. In the SS-DECT group, the population consisted of 17 female and 34 male patients with a mean age of 63 ± 12 years while in the DS-DECT group, the population consisted of 13 female and 38 male patients with a mean age of 64 ± 11 years.

Patient characteristics for both groups are shown in Table 2.

Table 2 Patient characteristics in the single-source dual-energy CT (SS-DECT) and dual-source dual-energy CT (DS-DECT) groups

	SS-DECT	DS-DECT
Age in years	62 ± 12 (range 36–91)	64 ± 11 (range 42–80)
Male/female	38/13 (75%/25%)	34/17 (67%/33%)
Nasopharyngeal cancer	4 × (8%)	3 × (6%)
Oropharyngeal cancer	16 × (31%)	19 × (37%)
Oral cavity cancer	15 × (29%)	14 × (27%)
Hypopharyngeal cancer	11 × (22%)	9 × (18%)
Laryngeal cancer	5 × (10%)	6 × (12%)

SS-DECT single-source dual-energy CT, *DS-DECT* dual-source dual-energy CT

Objective image analysis

Phantom experiment

The comparative CNRD in a 16-cm phantom with a central probe containing 35 mg iodine/mL was 11.7 $mGy^{-1/2}$ for SSDE and 14.3 $mGy^{-1/2}$ for DSDE using DI images, 16.7 $mGy^{-1/2}$ and 22.1 $mGy^{-1/2}$ using 60-keV VMI, and 21.9 $mGy^{-1/2}$ vs. 28.3 $mGy^{-1/2}$ using 40-keV VMI.

Vessel attenuation

With SS-DECT, the highest contrast and CNRD were at 40 keV, but due to the increase in image noise, CNRD was comparable with 60-keV VMI ($p = 0.24$); 40 keV was significantly higher than the DI ($p < 0.01$). Sixty-kiloelectron volt reconstructions were comparable to the DI ($p = 0.08$).

Compared to SS-DECT, CNRD values were 29% higher at 40 keV, 34% higher at 60 keV, and 37% higher on the DI with DS-DECT. CNRD values for both groups are shown in Table 3.

Tumor attenuation

In both groups, CNRD values at 40 keV were significantly higher than those at 60 keV and on the DI (all $p < 0.01$).

Compared to SS-DECT, CNRD values were 2% higher at 40 keV, 9% higher at 60 keV, and 13% higher on the DI with DS-DECT which was not statistically significant. Examples are shown in Fig. 1.

Subjective image analysis

Overall interrater agreement was substantial in the SS-DECT and in the DS-DECT groups (kappa value 0.63 and 0.77).

Tumor margin

In the SS-DECT group, no significant difference was found between 40 keV, 60 keV, and the DI. In the DS-DECT group, 40 keV had the highest mean rank score and was significantly better than the DI ($p = 0.003$) but comparable to 60 keV ($p = 0.67$). Forty kiloelectron volts and the DI were significantly better in the DS-DECT group compared to the SS-DECT group ($p = 0.02$ and 0.03).

Tumor contrast

In the SS-DECT group, 40 keV and 60 keV were significantly better than the DI ($p = 0.004$ and 0.02) while in the DS-DECT group, 40 keV was significantly better than 60 keV and the DI ($p = 0.02$ and < 0.01). Forty kiloelectron volts and the DI were

Table 3 CNR/CNRD values for SS-DECT and DS-DECT

	DS-DECT Tumor	SS-DECT Tumor	*p* value	DS-DECT Jugular vein	SS-DECT Jugular vein	*p* value
40 keV	8.45/4.20	8.33/4.12	0.802/0.975	28.20/6.92	20.56/5.03	0.001/0.005
60 keV	6.15/3.07	5.67/2.81	0.904/0.839	21.97/5.39	16.52/4.04	0.002/0.018
DI	4.36/2.16	3.86/1.91	0.352/0.439	17.70/4.34	13.15/3.22	0.002/0.012

DS-DECT dual-source dual-energy CT, *SS-DECT* single-source dual-energy CT, *DI* default images

rated significantly better in DS-DECT than the corresponding reconstructions in the SS-DECT group ($p = 0.007$ and < 0.01).

Artifacts

Shoulders In the SS-DECT group, the DI was significantly better than 40 keV and 60 keV (both $p < 0.01$). In the DS-DECT group, the DI was comparable to 60 keV ($p = 0.78$) but significantly better than 40 keV ($p < 0.01$). All reconstructions (40 keV, 60 keV, and the DI) were significantly better in the DS-DECT group compared to the SS-DECT group (all $p < 0.01$). Examples are shown in Fig. 2.

Oral cavity In the SS-DECT group, the DI was significantly better than 40 keV and 60 keV (both $p < 0.01$). In the DS-DECT group, results were comparable with the DI being significantly better than 40 keV and 60 keV ($p < 0.01$ and 0.04).

Pharynx In the SS-DECT, the DI was significantly better than 40 keV and 60 keV ($p =$ both 0.03). Main reason for poor ratings in monoenergetic images was artifacts at the edge between mucosa and air that increased with lower monoenergetic voltages. These artifacts were not found in the DS-DECT group. Examples are shown in Fig. 3.

Basal brain parenchyma In the SS-DECT group, the DI was significantly better than 40 keV and 60 keV ($p =$ both < 0.01). Main reason for poor ratings in monoenergetic images was a patchy and inhomogeneous visualization of the brain parenchyma that increased with lower monoenergetic voltages. These artifacts were not found in the DS-DECT group.

Overall subjective image quality

In the SS-DECT group, the DI was significantly higher compared to 40 keV ($p = 0.02$) but comparable to 60 keV ($p = 0.8$).

In the DS-DECT group, 40 keV had the highest image quality, significantly better than the DI ($p = 0.02$) but comparable to 60 keV ($p = 1.0$). Forty kiloelectron volts and 60 keV were significantly better than their corresponding reconstructions in the SS-DECT group (both $p < 0.01$) with no significant difference for the DI ($p = 0.47$).

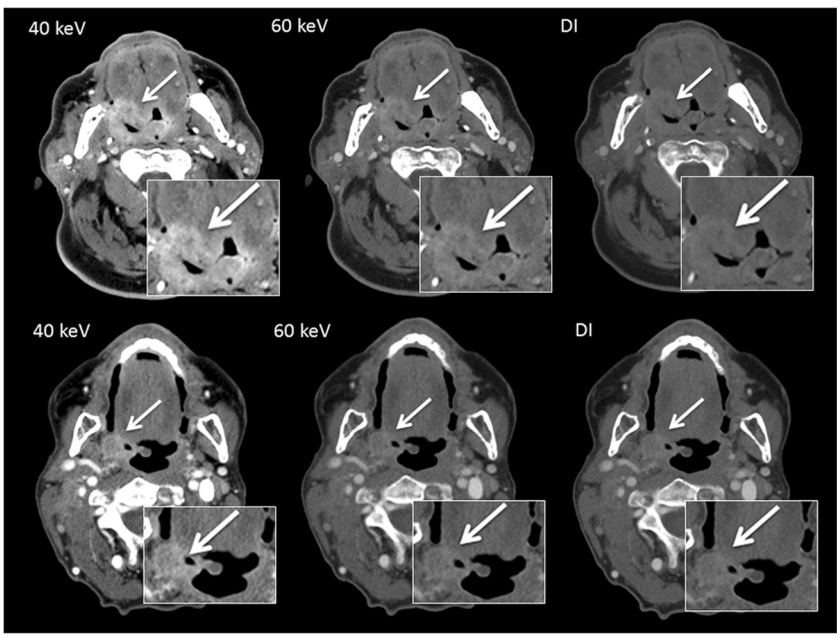

Fig. 1 Tumor delineation with both dual-energy techniques. Seventy-five-year old male patient with a cT4N1 carcinoma of the oropharynx on the right side who underwent SSDE (top row) and 59-year-old male patient with a cT2N2b carcinoma of the oropharynx on the right side who underwent DSDE (bottom row). Virtual monoenergetic reconstructions (40 keV, 60 keV) in comparison to default images (DI). All images are shown in the same window setting (W = 600 HU, C = 150 HU). Tumor delineation increases substantially with low-energy reconstructions for both techniques

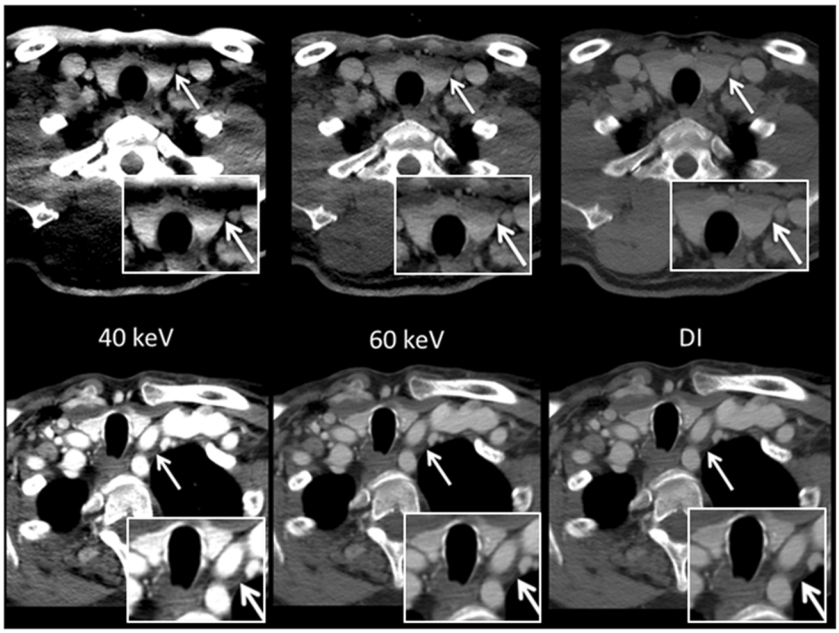

Fig. 2 Artifacts found at the level of the shoulders with both dual-energy techniques. Fifty-four-year old male patient with a cT1N0 carcinoma of the hypopharynx on the right side who underwent SSDE (top row) and 59-year-old male patient with a cT2N1 carcinoma of the oropharynx on the left side who underwent DSDE (bottom row). Virtual monoenergetic reconstructions (40 keV, 60 keV) in comparison to default images (DI). All images are shown in the same window setting (W = 600 HU, C = 150 HU). Image quality is significantly better with DI compared to both virtual monoenergetic reconstructions with both DE techniques. Artifacts are most pronounced on the 40-keV image with SSDE

Radiation exposure

$CTDI_{vol}$ was not significantly different between both examinations (SS-DECT 17.1 ± 1.6 mGy, DS-DECT 18.4 ± 3.9 mGy; $p = 0.3$). DLP (SS-DECT 496 ± 69 mGy cm, DS-DECT 587 ± 135 mGy cm) and ED (SS-DECT 2.5 ± 0.4 mSv, DS-DECT 3.0 ± 0.7 mSv) were significantly higher in DS-DECT because of higher mean scan lengths (SS-DECT 29.1 cm, DS-DECT 31.6 cm).

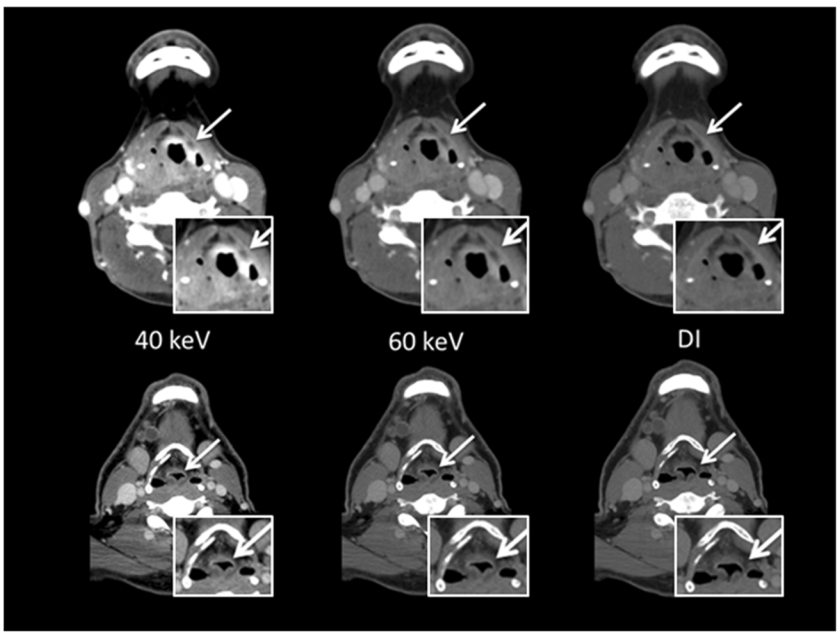

Fig. 3 Artifacts found in the pharynx with both dual-energy techniques. Forty-nine-year old female patient with a cT2N2b carcinoma of the hypopharynx on the right side who underwent SSDE (top row) and 62-year-old male patient with a cT2N0 carcinoma of the oral cavity on the left side who underwent DSDE (bottom row). Virtual monoenergetic reconstructions (40 keV, 60 keV) in comparison to default images (DI). All images are shown in the same window setting (W = 600 HU, C = 150 HU). Newly induced artifacts in the pharynx are only found on the 40-keV images with SSDE. These artifacts were never found with DSDE

Discussion

Recently introduced SS-DECT with a split-filter technique is applicable for staging examinations of the head and neck region. The best objective image quality for tumor evaluation could be obtained at 40 keV while subjective image quality at 40 keV was degraded by artifacts which were less pronounced at 60 keV and especially on the DI. Objective and subjective image quality was higher with DS-DECT.

The neck region suffers from low native contrast between soft tissues and virtually always contrast medium is applied for staging examinations. Dual energy offers the opportunity to increase the contrast to noise ratio by low monoenergetic reconstructions to improve the diagnostic image quality. The split-filter technique in SS-DECT was recently introduced and clinical data about this new application is scarce [6]. For both scanners, highest vessel CNRD values were obtained at the lowest keV setting available if advanced monoenergetic reconstruction algorithms are used, which seems to be in good agreement to other SS-DECT techniques [12]. While we found the best overall image quality on the DI, Lam et al published best results for rapid kV-switching for 65 keV. In our study, the phantom experiment reveals that DS-DECT outperformed SS-DECT as shown by the CNRD values for DI and 40 and 60 keV VMI. This finding aligns well with the results of patient image analysis (vessel attenuation). Vessel CNRD with DS-DECT is one-third higher than with SS-DECT, which is likely due to the superior spectral separation. These results are in line with a previous phantom study from Almeida et al [13] who also compared third-generation DS-DECT to third-generation SS-DECT equipped with the split-filter technique and reported that spatial resolution was equivalent but CNR was on average 1.4 higher.

The superior spectral separation and temporal coherence in DS-DECT also seem to account for the significantly lower image artifacts in the shoulder region. In both study groups, lower keV reconstructions led to increasingly pronounced artifacts compared to the DI which is attributable to photon starvation. Interestingly in the oral cavity, SS-DECT and DS-DECT reached comparable image quality regarding artifacts. We speculate that these artifacts caused by dental hardware might be too pronounced to achieve good image quality, no matter which CT scanner is used. High keV reconstructions (e.g., 190 keV) can be used to reduce metal artifacts; however, a known limitation of this approach is the loss of iodine contrast at high keV. For tumor and vessel evaluation, this leads to non-diagnostic or limited diagnostic images [1]. Highest vessel and tumor contrast can be achieved with low keV reconstructions (40 keV) but image quality in the oral cavity is hampered by more pronounced metal artifacts. Thus, the selection of keV reconstructions always presents a trade-off between artifacts and tumor visualization. Other options to improve image quality are dedicated metal artifact reduction algorithms or an additional examination aligned to the jaw with a limited scan range [14].

In SS-DECT, newly induced artifacts were also found in the basal slices of the brain parenchyma and in the pharynx at the transition zone between air and soft tissue structures. These artifacts were mainly found on 40-keV reconstructions and to a much lesser degree on 60 keV. These artifacts were not yet described in the previously published studies using DS- or SS-DECT.

Limitations

Some limitations need to be stated.

First, both groups consisted of different patients and data would be more comparable if SS-DECT and DS-DECT scans could have been performed in the same patient, but this was ethically not justifiable. Therefore, especially the comparison of subjective tumor reproduction between the both groups should be interpreted carefully.

Second, we used vendor-specific presets for the inline DI in both groups that in the case of SS-DECT also cannot be changed by the user. However, these presets could be considered as standard settings and only show slight differences in mixing ratios and specific algorithms.

Third, the dual-energy technique of only one vendor could be evaluated. Therefore, no direct comparisons to other dual-energy imaging algorithms are possible.

Forth, SS- and DS-DECT use different hard- and software and many confounding factors cannot be matched between both techniques. Especially different detector geometries lead to different effects concerning radiation dose like scattered radiation and overscanning that are only reflected by the CTDIvol given from the scanner. Therefore, we sought to overcome this limitation by providing the CNRD as a figure of merit. Nevertheless, our study provides important information how both techniques compare to each other in clinical routine with the current specifications available.

Conclusion

In single-source CT equipped with split filter, the combination of DI and low keV reconstructions seems to be the best compromise between CNRD and imaging artifacts. Third-generation dual-source CT is superior to single-source CT with split-filter technique in terms of image quality.

Funding The authors state that this work has not received any funding.

Compliance with ethical standards

Guarantor The scientific guarantor of this publication is Wolfgang Wuest.

Conflict of interest The authors of this manuscript declare relationships with the following companies: Rafael Heiss, Marco Wiesmueller, Michael Uder, Matthias Stefan May, and Wolfgang Wuest are members of Siemens Healthcare GmbH speakers' bureau.

Statistics and biometry One of the authors has significant statistical expertise.

Informed consent Written informed consent was obtained from all subjects in this study.

Ethical approval Institutional Review Board approval was obtained.

Methodology
- prospective
- cross-sectional study
- performed at one institution

References

1. May MS, Bruegel J, Brand M et al (2017) Computed tomography of the head and neck region for tumor staging-comparison of dual-source, dual-energy and low-kilovolt, single-energy acquisitions. Invest Radiol 52(9):522–528
2. McCollough CH, Leng S, Yu L, Fletcher JG (2015) Dual- and multi-energy CT: principles, technical approaches, and clinical applications. Radiology 276(3):637–653
3. Wichmann JL, Nöske EM, Kraft J et al (2014) Virtual monoenergetic dual-energy computed tomography: optimization of kiloelectron volt settings in head and neck cancer. Invest Radiol 49:735–741
4. Scholtz JE, Kaup M, Kraft J et al (2015) Objective and subjective image quality of primary and recurrent squamous cell carcinoma on head and neck low-tube-voltage 80-kVp computed tomography. Neuroradiology 57:645–651
5. Toepker M, Czerny C, Ringl H et al (2014) Can dual-energy CT improve the assessment of tumor margins in oral cancer? Oral Oncol 50(3):221–227
6. Faby S, Kuchenbecker S, Sawall S et al (2015) Performance of today's dual energy CT and future multi energy CT in virtual non-contrast imaging and in iodine quantification: a simulation study. Med Phys 42(7):4349–4366
7. Kaemmerer N, Brand M, Hammon M et al (2016) Dual-energy computed tomography angiography of the head and neck with single-source computed tomography: a new technical (split filter) approach for bone removal. Invest Radiol 51(10):618–623
8. Euler A, Parakh A, Falkowski AL et al (2016) Initial results of a single-source dual energy computed tomography technique using a split-filter: assessment of image quality, radiation dose, and accuracy of dual-energy applications in an in vitro and in vivo study. Invest Radiol 51:491–498
9. Uhrig M, Simons D, Kachelrieß M, Pisana F, Kuchenbecker S, Schlemmer HP (2016) Advanced abdominal imaging with dual energy CT is feasible without increasing radiation dose. Cancer Imaging 16(1):15
10. Deak PD, Smal Y, Kalender WA (2010) Multisection CT protocols: sex- and age-specific conversion factors used to determine effective dose from dose-length product. Radiology 257:158–166
11. Landis JR, Koch GG (1977) The measurement of observer agreement for categorical data. Biometrics 33(1):159–174
12. Lam S, Gupta R, Levental M, Yu E, Curtin HD, Forghani R (2015) Optimal virtual monochromatic images for evaluation of normal tissues and head and neck cancer using dual-energy CT. AJNR Am J Neuroradiol 36(8):1518–1524
13. Almeida IP, Schyns LE, Öllers MC et al (2017) Dual-energy CT quantitative imaging: a comparison study between twin-beam and dual-source CT scanners. Med Phys 44(1):171–179
14. Wuest W, May MS, Brand M et al (2015) Improved image quality in head and neck CT using a 3D iterative approach to reduce metal artifact. AJNR Am J Neuroradiol 36:1988–1993